Petroleum Science 23 (2026) 966–978

Contents lists available at ScienceDirect

Petroleum Science

journal homepage: www.keaipublishing.com/en/journals/petroleum-science

Original Paper

Comparing the thermal processing with slurry phase hydroupgrading to increase the yields of distillates of Arabian heavy crude oil

Yi-Di Wang [a,b], Xu Zhang [a,b], Xin-Yi Feng [c], Bin Liu [a,b], Yuan Pan [a], Guang-Zheng Sun [a,b], Hong-Yang Lv [a,b], Feng-Yu Tian [a,b], Bin Dong [a], Yi-Chuan Li [a], Chen-Guang Liu [a,b], Yong-Ming Chai [a,b,*]

[a] State Key Laboratory of Heavy Oil Processing, College of Chemistry and Chemical Engineering, China University of Petroleum (East China), Qingdao, 266580, Shandong, China
[b] Key Laboratory of Catalysis, China National Petroleum Corporation (CNPC), Qingdao, 266580, Shandong, China
[c] Schlumberger Ltd., Tianjin, 300452, China

ARTICLE INFO

Article history:
Received 17 March 2025
Received in revised form
9 August 2025
Accepted 17 November 2025
Available online 20 November 2025

Edited by Min Li

Keywords:
Slurry phase hydroupgrading
Crude oil pretreatment
Asphaltene
Heteroatom compounds
Reaction mechanism

ABSTRACT

With the increasing heavy and inferior quality of global oil resources, the efficient utilization of crude oil has become a critical challenge to be solved in the energy field. This work intends to propose a feasible way of crude oil pretreatment in the refining process. A comparison of the comprehensive performance differences between thermal processing (TP) and slurry phase hydroupgrading (SPH) treatments revealed that SPH had a great upgrading effect for Arabian heavy crude oil under 390 °C and oil-soluble MoS_2 catalyst. Compared with the feedstock, the asphaltene content of TP product increased by 13.2 wt%, that in SPH product dropped by about 19.8 wt%. And the total distillate yield (≤540 °C) of SPH increased by 4.4 wt% compared to the TP. The results of SARA separation and X-Ray Diffraction (XRD) showed that SPH can not only inhibit the occurrence of free radical reactions, but also dissociate the original asphaltene. The detailed composition of the processed samples was characterized by gas chromatography-mass spectrometry (GC-MS) and electrospray ionization orbitrap mass spectrometry (ESI Orbitrap MS) to explore the molecular transformation mechanism of different processes. There are a considerable number of –S– bonds in asphaltene as important structural connection hubs. The process of SPH can promote the production of light hydrocarbons while effectively removing heteroatom compounds. Finally, we considered that it is necessary to carry out the SPH pretreatment for Arabian heavy crude oil.

1. Introduction

Crude oil plays a vital role in the evolution of human civilization, and it still occupies a dominant position in the world energy system (Liu et al., 2024b). Under the dual drivers of oil price and technological advancements, a large number of low-grade reserves and unconventional oil resources have been gradually put into development, primarily including tight oil, extra-heavy oil (oil sands, bitumen) and so on (Guo et al., 2016; Sun et al., 2025; Zhu et al., 2024). According to projections by the International Energy Agency (IEA), the proportion of global heavy oil reserve within total petroleum resource is exhibiting an upward trend, with the majority concentrated in Venezuela (the largest holder of heavy oil reserves), Canada, Russia, and the Middle East (Pham et al., 2024; Wang et al., 2024; Zheng et al., 2024).

With the continuous innovation in petroleum exploration and development technologies, the exploitation efforts for heavy crude oil resources are expected to intensify, which is gradually becoming the focus of the refining industry. Heavy oil plays a significant yet complex role in the refining process due to its characteristics of high density, viscosity, heteroatom content, and heavy metal concentration. The essence of refining process related

* Corresponding author.
E-mail address: ymchai@upc.edu.cn (Y.-M. Chai).
Peer review under the responsibility of China University of Petroleum (Beijing).

https://doi.org/10.1016/j.petsci.2025.11.032

to the order of technologies involved in the process of transformation of the crude oil into finish marketable products has the potential of considerable improvement of refining profitability. The core processes of refinery mainly include crude distillation unit (CDU), hydrotreating, reforming, alkylation and isomerization processes, etc. As the first step of crude oil processing, CDU is used to separate components with different boiling point ranges in crude oil and provide feedstocks for subsequent processing (Khafaji et al., 2024; Stratiev et al., 2024). However, as global crude oil resources increasingly exhibit trends toward heavier and more inferior quality, leading to a growing impact from asphaltene and heteroatom compounds. In generally, asphaltene is insoluble in low grade *n*-alkanes and soluble in aromatic solvents such as benzene and toluene (Liang et al., 2024; Marquez et al., 2024). Berg (2022) systematically reviewed the development of solvent titration techniques for asphaltene, specifically those based on using two solvents. It enhanced our understanding of asphaltene characteristics. In molecular simulation, asphaltene is divided into "archipelago" and "island" models according to the number of aromatic fused ring cores (Chacón-Patiño et al., 2018; Law et al., 2019; Meng et al., 2023). Dickie and Yen (1967), Mullins (2010), and Yen et al. (1961) proposed the Yen-Mullins hierarchical structure model, this model shows that the aggregation of asphaltene includes three levels. Gray et al. (2011) proposed a supramolecular model of asphaltene, asphaltene aggregation is a stable supramolecular structure formed by a variety of intermolecular interactions. Although the molecular structure of asphaltene is not clear at present, a large number of studies have shown that it is easy to associate between molecules by interaction, which has a serious negative impact on oil exploitation, storage, transportation and processing (Adeyanju and Oyekunle, 2019; Kamkar and Natale, 2021; Moon et al., 2024). Non-covalent interaction is the dominant factor of asphaltene aggregation, which is mainly divided into two categories: The first type is represented by electrostatic interaction, such as hydrogen bonds formed by polar groups on the side chain (He et al., 2022; Khalaf and Mansoori, 2018); The second type is represented by dispersion interaction, such as π-π stacking interaction between polycyclic aromatic hydrocarbons, σ-π interaction between aliphatic side chains and aromatic rings, and σ-σ interaction between long side chains (Bian et al., 2021; He et al., 2022). The heteroatom compounds in petroleum mainly include sulfur compounds, nitrogen compounds and oxygen compounds, which pose significant hazards to the refining process and the quality of related petroleum products (Deng et al., 2024; Li et al., 2023). Sulfur compounds tend to generate corrosive gas (H_2S) during processing, damaging pipelines and equipment, while also poisoning catalysts and reducing the activity of key reactions such as cracking and reforming (Wang et al., 2023b; Wu et al., 2023). Furthermore, nitrogen compounds not only inhibit the efficiency of hydrodesulfurization (HDS) reactions, increasing the difficulty of sulfur removal, but also affect fuel stability and contribute to environmental pollution by generating nitrogen oxides (NO_x) (Lu et al., 2025). Additionally, oxygen compounds can form acidic substances to accelerate equipment corrosion during processing and polymerize to form coke, clogging reactors and increasing refining costs.

Therefore, it is the key to ensure the efficient operation of the subsequent process to use appropriate methods to pretreat undesirable components (asphaltene, heteroatom compounds) in heavy crude oil before CDU to achieve initial quality improvement. Thermal processing (TP) and slurry phase hydroupgrading (SPH) treatments serve as pivotal technologies for heavy oil upgrading, demonstrating significant application value in petroleum refining (Lu et al., 2025; Wang et al., 2022, 2023a). TP treatment is a conventional refining process that converts heavy oils into lighter fractions through high temperature treatment (>400 °C). Its fundamental mechanism involves utilizing thermal energy to induce bond cleavage reactions in large hydrocarbon molecules of petroleum (Wang et al., 2022). However, TP exhibits technical limitations such as poor product selectivity and severe coking tendency, restricting its applications to specialized areas like heavy oil processing. SPH has strong adaptability to feedstock, which is the most important way to efficiently utilize heavy oil (Wang et al., 2023a). Its technical core is to efficiently convert polycyclic aromatic hydrocarbons such as asphaltene and inhibit coke formation, while removing heteroatom compounds from petroleum (Al-Attas et al., 2019; Mateus-Rubiano et al., 2024; Mishra et al., 2025; Prajapati et al., 2021; Yuan et al., 2025). Homogeneously dispersed catalysts are generally used in the hydrogenation process (Hai Pham et al., 2022). The catalysts can be directly dispersed in oil to enhance the hydrogenation reaction activity and overcome the disadvantages about significant pressure decrease when using ebullated or fixed-bed reactors (Al-Attas et al., 2019). Although there are many types of catalyst available for SPH, the oil-soluble molybdenum-containing catalyst has been widely used in industrial production. It has several advantages such as simple preparation and high hydrogenation activity (Chen et al., 2022a; Wang et al., 2021; Liu et al., 2019, 2024a; Luo et al., 2022). Additionally, Usman et al. (2017) mixed Arab Extra Light (AXL) crude oil with its liquid product in different proportions. The mixed feedstock was subsequently subjected to catalytic cracking treatment, yielding light olefins comparable to those obtained from direct crude oil cracking. This route provides alternative innovative strategies for treating crude oil.

SPH can maximize the conversion of heavy components (residual oil) and the yield of light components (liquid product) (Browning et al., 2019; Chen et al., 2022a; Feng et al., 2022; Hai Pham et al., 2022). In view of the high degree of polymerization and strong steric hindrance for asphaltene, there are few effective approaches to analysis. The difficulty of subsequent analysis can be greatly decreased after asphaltene dissociation by SPH. The hydrogenation process can reduce the formation of asphaltene precipitates and improve the structure of asphaltene. Yang et al. (2022) and Prajapati et al. (2021) elaborated on the evolution of asphaltene, in which the occurring of hydrogen and catalyst can inhibit the aggregation of asphaltene and prevent excessive cracking while breaking alkyl chains. Different types of catalyst have different hydrogenation effects, and SPH of crude oil provides a preliminary cognition of the coking mechanism for asphaltene (Rawat et al., 2024). On the other hand, the presence of heteroatom compounds also significantly degrades the properties of crude oil. The relevant standards of petrochemical industry have strict requirements on the content of heteroatoms in petroleum products. SPH has excellent ability to remove heteroatom compounds (Roy et al., 2021; Wang et al., 2023a). The research of the reaction mechanism for hydrodesulfurization (HDS) and hydrodenitrogenation (HDN) is helpful to improve the understanding of heteroatoms removal process (Bello et al., 2021). Chen et al. (2022b) analyzed the composition of sulfur species and the reactivity of HDS in deasphalted oils by high-resolution mass spectrometry (HRMS). In fact, the understanding of the reaction mechanism and transform for SPH is currently unclear for now due to the lack of the composition characterization of molecular level. It hinders the upgrading and application of SPH.

In recent years, the rapid development of petroleum analysis technology represented by HRMS makes it possible to understand the composition of crude oil and its derivatives (Su et al., 2023; Zhao et al., 2021). For low boiling point components, we can use GC-MS for analysis; for high boiling point components, we can use

HRMS to characterize their molecular composition. In addition, we can characterize various types of compounds such as hydrocarbon compounds, sulfur compounds, nitrogen compounds and oxygen compounds combined with relevant derivatization methods (Shi and Wu, 2021). Li et al. (2023, 2024) and Shi et al. (2021) have conducted quantitative analysis of the full molecular composition for crude oil, which has advanced the understanding of petroleum chemistry. In this work, we proposed that crude oil should be pretreated by SPH and proved that it has obvious lightweight and asphaltene dissociation effect. The detailed composition of crude oil in the TP and SPH treatments were characterized at a molecular level to explore the transformation mechanism of different processes. Semi-quantitative analysis of hydrocarbons and heteroatom compounds were carried out by GC-MS and Orbitrap MS to further explain the reaction law of the hydroupgrading process. This offers constructive guidance for the refining process.

2. Experimental section

2.1. Materials and reagents

Analytical-grade methanol, toluene, dichloromethane (DCM), and *n*-hexane (*n*-C6) were obtained from Beijing Chemical Reagents Company. Analytical-grade petroleum ether was obtained from Shanghai Titan Scientific Co., Ltd. The solvents were distillated by a B/R 9600 spanning band distillation instrument (B/R Instrument Corporation, USA) before use. Silver tetrafluoroborate ($AgBF_4$) and methyl iodide (MeI) were purchased from J&K Chemical Ltd.

The Arabian heavy crude oil used in the experiments was obtained from Sinopec Group. Five oil-soluble catalysts with different metals (Mo, Ni, Co, Fe and Cu) were prepared and their hydroupgrading performance was investigated. The method of preparing has been described in the Supporting Information.

2.2. Thermal processing and slurry phase hydroupgrading treatments

The objective of this work is to combine research results with actual production, providing theoretical support for refinery improvement. According to research studies, China currently operates a large number of major refineries, and its refining capacity ranks among the top globally (Li et al., 2025; Liu et al., 2020). The feedstock of domestic refineries in China primarily comes from Middle Eastern countries, including Saudi Arabia, the UAE, Iran, and Iraq. The demand of Saudi crude oil is the highest among them, which can create significant economic benefits. Therefore, Arabian heavy crude oil was chosen as the object of this work to confirm the necessity of SPH pretreatment.

In order to explore the suitable process conditions, the hydroupgrading performance of five different oil-soluble catalysts was evaluated. Secondly, the Saudi crude oil was hydrogenated at different temperatures, including 330, 350, 370, 390 and 410 °C. Finally, the most suitable temperature condition of SPH was selected to conduct TP treatment of Saudi crude oil for upgrading effect comparison. Fig. 1 shows the schematic diagram of TP and SPH treatments. These two processes were experimented in batch reactor and continuously fed with N_2 and H_2, respectively. In this paper, the unprocessed Saudi crude oil was named ST-1; The Saudi crude oil after TP treatment was named ST-2; The Saudi crude oil after hydroupgrading treatment was named ST-3, which was used to represent the process of SPH.

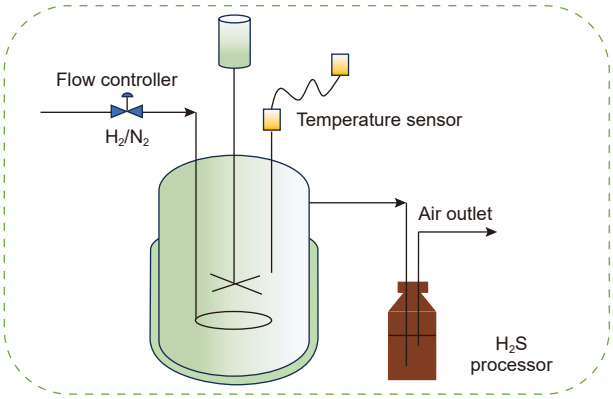

Fig. 1. Experimental installation of crude oil processing. N_2 and H_2 are used in TP and SPH treatments, respectively.

3. Methodology

3.1. Bulk properties and XRD analysis

The total nitrogen and sulfur contents of samples and their fractions were analyzed using a Multi Vario EL III sulfur/nitrogen analyzer (Elementar, Germany) according to ASTM D5453 and ASTM D5762, respectively. The total carbon and hydrogen contents were analyzed using a Vario EL cube elemental analyzer (Elementar, Germany) according to ASTM D5291. Density and viscosity were analyzed by Chinese industry standards SH/T 0604 and GB/T 265, respectively. The simulated distillation curve of the feedstock and processed samples were analyzed according to ASTM D7213. The saturates, aromatics, resins and asphaltenes were obtained by SARA separation according to Chinese industry standard NB/SH/T 0509–2010 which was equivalent to ASTM D2007-93.

X-ray powder diffraction (XRD) patterns of the asphaltene were investigated by a PANalytical's X'Pert PRO diffractometer using Cu-Kα radiation operated at 45 kV and 40 mA with the scan rate of 5 °/min and 2θ range of 5°–75°.

3.2. GC-MS analysis

A Thermo Scientific Trace 1310 GC coupled with a Thermo Scientific TSQ 8000Evo MS was used for the analysis of SARA separation samples. The GC was equipped with a HP-5MS (60 m × 0.25 mm × 0.25 μm) fused silica capillary column. For saturate fraction analysis, the oven temperature was programed from 50 to 120 °C at 20 °C/min, from 120 to 250 °C at 4 °C/min and 250–310 °C at 3 °C/min with an initial hold time of 1 min and a final hold time of 30 min. For aromatic fraction analysis, the oven temperature was programed from 50 to 120 °C at 15 °C/min and 120–300 °C at 3 °C/min with an initial hold time of 1 min and a final hold time of 35 min. The energy of electron impact ion (EI) source was 70 eV and it was operated at 230 °C. The mass range of saturate fraction analysis was from *m/z* 35 to *m/z* 600 with a scan period of 0.6 s and aromatic fraction analysis was from *m/z* 35 to *m/z* 420 with 0.92 s, respectively.

3.3. ESI orbitrap MS analysis

The molecular composition of all samples was characterized by an Orbitrap Fusion MS (Thermo Scientific, USA). The ion transfer tube temperature was 300 °C, and the detection mass range was *m/z* 100–1000, the cumulative number of ions (AGC target) was approximately 1.0×10^6 within a cumulative time of 100 ms. ESI

was carried out in negative-ion or positive-ion modes. The prepared samples were injected into ESI through an automatic peristaltic pump at a flow rate of 8 μL/min. The spray voltages were −2.6 and 3.6 kV, sheath gas flow rates were 5 or 8 arbitrary units, auxiliary flow rates were 2 or 3 arbitrary units for two ionization modes, respectively.

4. Results and discussion

4.1. Condition establishment and property analysis

Fig. 2(a) shows the fraction composition of hydroupgrading products under different catalysts. The reaction condition of temperature and pressure were 390 °C and 7 MPa, respectively. The hydroupgrading activity of Mo is stronger than other metals. The proportion of gas is only 0.9 wt%, which means that the cracking reaction was effectively suppressed. The generation efficiency of hydrogen radical was better than that of other metals. Compared with the crude oil, the proportion of VR of Mo decreased from 34.6 to 26.1 wt%, which was the lowest of all metals. The light fraction proportion increased significantly, the change of AGO content was the most obvious. In our previous work, we developed an oil-soluble MoS_2 catalyst for SPH and it has achieved industrial application (Liu et al., 2019; Tian et al., 2024; Wang et al., 2023a). We decided to do the next work on this basis.

Fig. 2(b) shows the fraction composition of hydroupgrading products with oil-soluble MoS_2 catalyst under different temperatures. With the increase of temperature, the hydroupgrading effect was gradually enhanced. And the change of gas content showed the same trend. We can see that the 390 °C is a turning point of fraction composition of hydroupgrading products. The proportion of liquid fractions at 390 °C is essentially the same as that at 410 °C. However, the proportion of gas increased from 0.9 wt% to 1.3 wt%. In addition, the formation of coke was also detected at 410 °C. It shows that the advantages of free radical reaction began to gradually appear, which is not what we want. The reaction time, pressure and catalyst concentration of SPH are consistent with those of industrial devices. The final selected experimental conditions of two processes are shown in Table 1.

The related bulk properties and SARA separation results of the feedstock and processed samples are shown in Table 2. It can be seen that the density and viscosity of feedstock are 0.8896 g/cm^3 and 22.68 mPa·s, respectively. And the contents of sulfur and nitrogen are 3.57 and 0.19 wt%, respectively. The former is almost 19 times that of the latter. The asphaltene content is as high as 9.1 wt% in the feedstock and Fig. 2(a) shows that the proportion of VR accounts for 34.6 wt%, indicating that the crude oil used in this study conforms to the characteristics of typical Arabian heavy crude oil (high sulfur). Compared with the feedstock, the density (20 °C) and viscosity (50 °C) of ST-2 and ST-3 were both significantly reduced. The sulfur content of ST-2 is basically the same as that of the feedstock, whereas the sulfur conversion of ST-3 achieves 15.5 wt%, indicating that SPH exhibits higher desulfurization efficiency than TP.

The results of SARA separation show that the content of asphaltene exhibited considerable variability. In order to ensure

Table 1
Reaction conditions of the TP and SPH treatments.

Sample	ST-2	ST-3
Process	TP	SPH
Reactor	Batch reactor	Batch reactor
Time, h	1	1
Temperature, °C	390	390
Gas atmosphere	N_2	H_2
Pressure, MPa	–	7
Catalyst	–	Oil-soluble MoS_2 catalyst
Catalyst concentration, μg·g^{-1}	–	1000

Table 2
Bulk properties and SARA separation of the feedstock and processed samples.

Sample	ST-1	ST-2	ST-3
Density (20 °C), g/cm^3	0.8896	0.8837	0.8847
Viscosity (50 °C), mPa·s	22.68	16.14	17.27
C, wt%	84.06	83.81	84.40
H, wt%	12.17	12.56	12.42
N, wt%	0.19	0.16	0.15
S, wt%	3.57	3.49	3.02
S_{asp}, wt%	8.48	8.04	8.84
Sat, wt%	45.8	45.2	47.8
Aro, wt%	27.7	27.2	28.5
Res, wt%	17.4	17.3	16.4
Asp, wt%	9.1	10.3	7.3

Note: S_{asp} represents the sulfur content in asphaltenes.

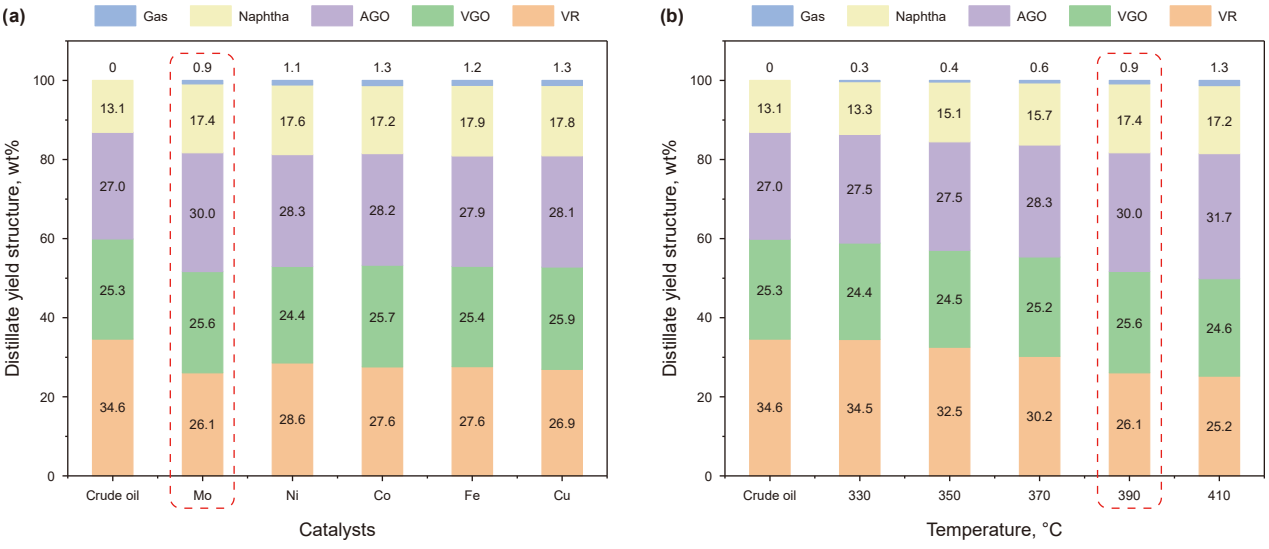

Fig. 2. Fraction composition of hydroupgrading products under **(a)** different catalysts and **(b)** different temperatures.

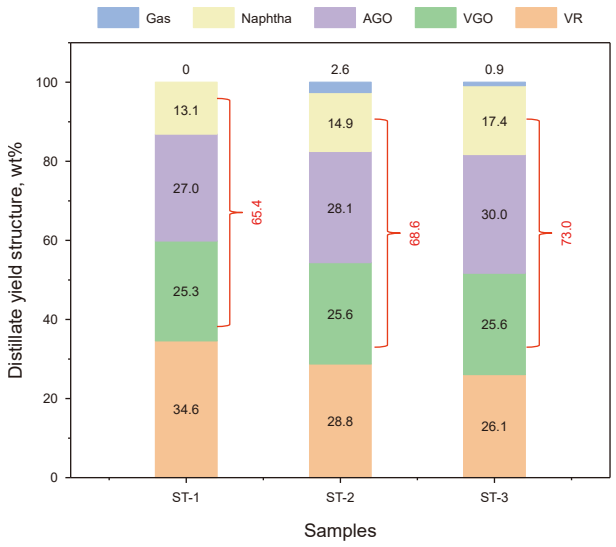

Fig. 3. Fraction composition of simulated distillation for the feedstock and processed samples. Note: ST-1 is the feedstock, ST-2 and ST-3 represent the samples obtained under 390 °C by TP and SPH treatments, respectively.

the precision of the separation method, three repeated experiments were performed for all samples, with the mean values being adopted as the final results. Compared with the feedstock, the asphaltene content of ST-2 increased from 9.1 to 10.3 wt%. This indicates that asphaltene aggregation can be formed in the process of TP. And the aggregation process follows the reaction mechanism of free radical. On the contrary, the content of ST-3 decreased to 7.3 wt%. The process of SPH can not only inhibit the occurrence of free radical reaction, but also dissociate the original asphaltene in crude oil, thereby reducing the content of heavy components. The content of saturates and aromatics in ST-2 are lower than ST-1, but ST-3 presents the opposite. This phenomenon provides evidence that hydrocarbons were transformed in the above reaction processes.

4.2. Distillation characteristics and asphaltene analysis of different samples

The fraction composition of the feedstock and processed samples can be found in Fig. 3. Compared with the feedstock, the proportion of light oil (≤540 °C) in ST-3 increased from 65.4 to 73.0 wt% and the proportion of VR decreased from 34.6 wt% to 26.1 wt%. This shows that the process of SPH has excellent lightweight effect. It is noteworthy that the properties of ST-2 also seem to be optimized, but this does not mean that the treatment effect of ST-2 for crude oil is good. Although the proportion of light component of ST-2 has increased, a large amount of gas (2.6 wt%) was generated during processing. Most importantly, the asphaltene content in ST-2 increased by 1.2 wt% compared to the feedstock as shown in Table 2. It indicates that the free radical reaction is uncontrollable in the process of TP. In addition, the proportion of light oil in ST-3 has been further improved compared to ST-2 which increased by 4.4 wt%. Therefore, it is necessary to pretreat crude oil by SPH.

The separated asphaltene components were analyzed by XRD. Fig. 4(a) shows the doublet γ peak at around 20° and broad peak (002) at about 26°, respectively. The occurrence of the doublet γ peak is due to aliphatic side chains and the broad peak (002) is due to condensed aromatic rings. The calculation method of crystalline parameters (La, M) in asphaltene referred to previous studies (Kovalenko et al., 2023; Rawat et al., 2024). The relevant equations are shown in the Supporting Information. As shown in Fig. 4(b), La and M represent the average diameter of the aromatic sheet and the number of aromatic sheets, respectively (Kovalenko et al., 2023; Rawat et al., 2024). The value of La and M for ST-2 (Asp) increased significantly compared with the ST-1 (Asp). La increased from 2.16 to 3.85 and M increased from 5.42 to 8.37. The value of La and M for ST-3 (Asp) are 0.97 and 4.67, which are much smaller than ST-1 (Asp) and ST-2 (Asp).

As mentioned above, it shows that the alkyl chains and aromatic ring lamellae developed in the direction of aggregation during the TP treatment. The polycyclic aromatic hydrocarbons in asphaltene entered the activation state of free radical by heating and reacted with other hydrocarbon free radicals, resulting in the association of asphaltene. The hydrogen radicals in the process of SPH can destroy the polycyclic aromatic hydrocarbon free radicals in time and terminate the free radical reaction in advance. Hydrogen radicals have strong activity, which can cause the breakage of chemical bonds (–S–, C–S) to decompose the aromatic structure and alkyl chains of asphaltene aggregation. The variations of M mean that the polycyclic aromatic hydrocarbon radicals reacted with each other but hydrogen radicals inhibited this process. Moreover, with the occurring of breakage reaction for alkyl chain and aromatic sheets, the internal space resistance of asphaltene would decrease. This promoted the removal of heteroatom compounds, such as sulfur compounds, nitrogen

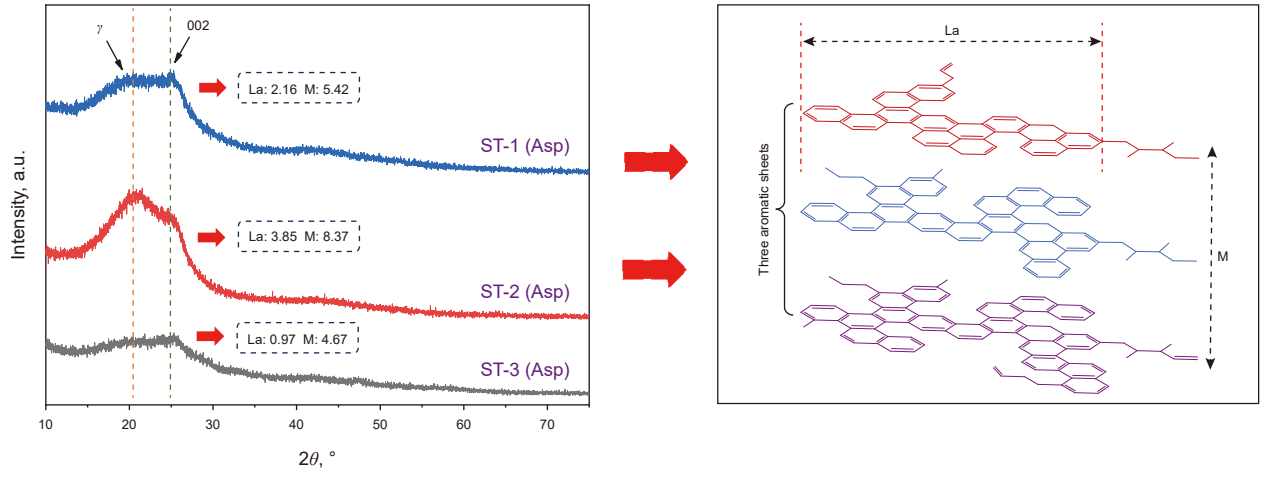

Fig. 4. **(a)** XRD analysis of asphaltene in different samples and **(b)** some crystalline parameters of asphaltene aggregation (Kovalenko et al., 2023; Rawat et al., 2024).

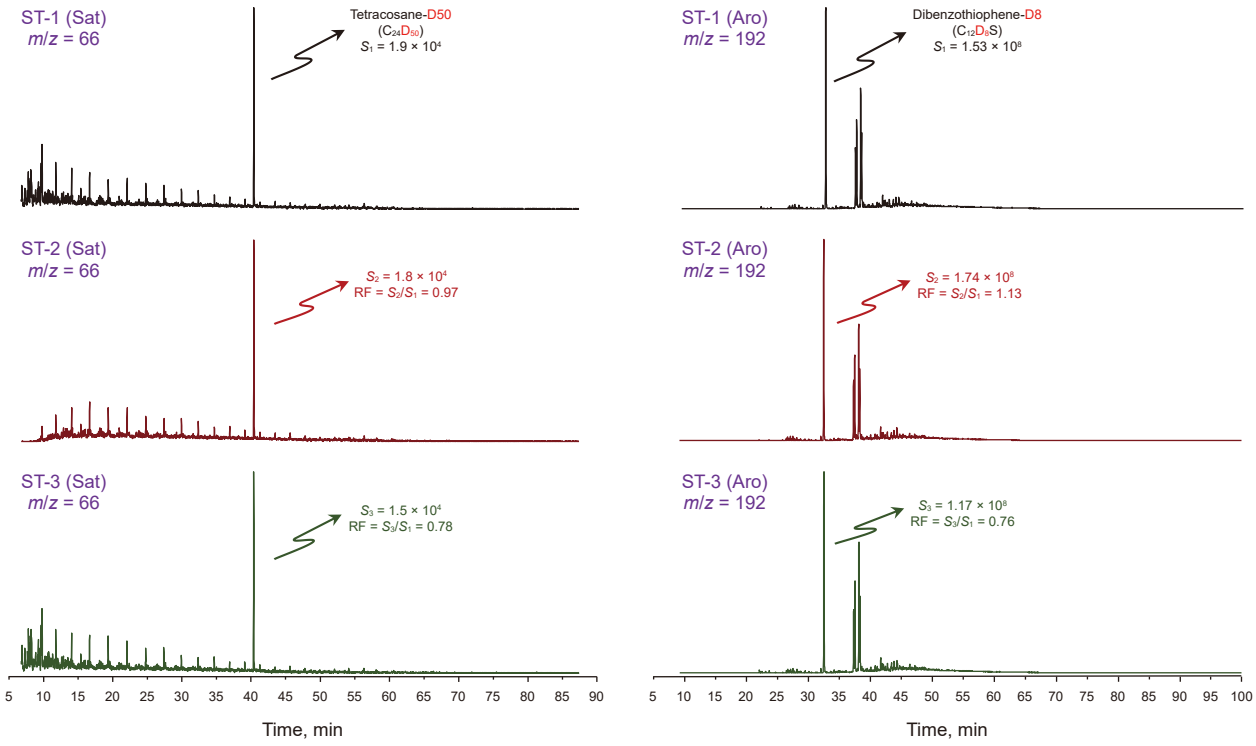

Fig. 5. GC-MS mass chromatograms of the internal standards in saturates and aromatics.

compounds and oxygen compounds. The discussion of heteroatom compounds will be reflected in the following content.

4.3. Semi-quantitative molecular composition of hydrocarbon fractions

The semi-quantitative analysis of saturates and aromatics in the feedstock and processed samples were analyzed by GC-MS with internal standard method. The total ion chromatograms (TIC) of saturates and aromatics can be found in Supporting Information. Fig. 5 shows the chromatographic peaks of internal standard in saturates and aromatics. And the structure of them can be found in Supporting Information. The response factor (RF) of different components was determined by the integral area of the internal standard peaks. The $C_{24}D_{50}$ was used as the internal standard compound of saturate. The RF of ST-2 (Sat) and ST-3 (Sat) are 0.97 and 0.78, respectively. The $C_{12}D_8S$ was used as the internal standard compound of aromatic. The RF of ST-2 (Aro) and ST-3 (Aro) are 1.13 and 0.76, respectively. In addition, the relative content (RC) of different compounds can be calculated by Eq. (1). In which RC is the relative content of compounds by processes compared with the feedstock; i represents any type compound; S is the integral area of compounds; S_0 is the integral area of corresponding compounds in ST-1; RF can be obtained in Fig. 5.

$$RC_i = \frac{S_i}{S_0} \times RF_i \quad (1)$$

Fig. 6 shows the change of *n*-alkanes in saturates. The *n*-alkanes of low carbon number (C9–C18) were obviously transformed in the

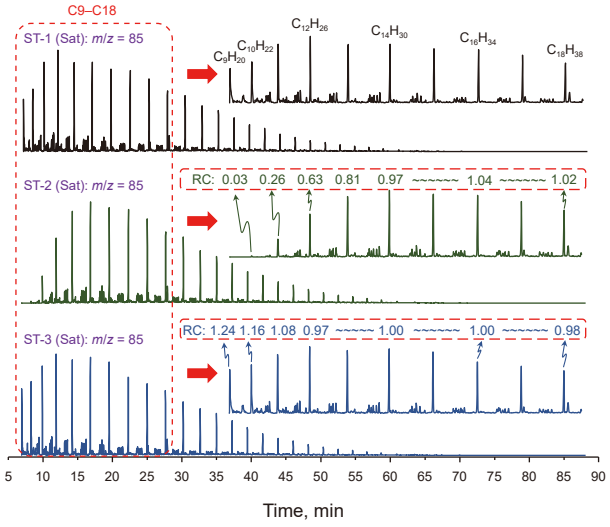

Fig. 6. GC-MS extracted ion chromatograms of *n*-alkanes in saturates.

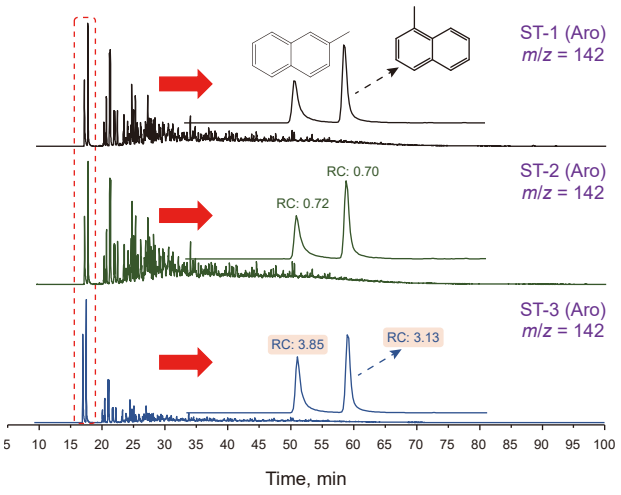

Fig. 7. GC-MS extracted ion chromatograms of methylnaphthalene in aromatics.

treatment process of TP. As we can see, the RC of *n*-alkanes before the $C_{13}H_{28}$ reduced with the decreasing of carbon number, in which the C_9H_{20} and $C_{10}H_{22}$ were basically completely converted. Because the experimental temperature of TP was formulated as 390 °C in this work, it cannot reach the breakage standard of C–C bonds of this part of small molecular *n*-alkanes but the free radical reactions tend to occur at this time. Combined with the SARA separation results and asphaltene characterization data, it can be seen that this part of the converted n-alkanes reacted with the free radicals of polycyclic aromatic hydrocarbons in asphaltene by chain initiation. The RC of *n*-alkanes with high carbon number (>C14) is consistent with the feedstock. This means that these *n*-alkanes did not participate in the aggregation reaction.

On the contrary, the *n*-alkanes were not consumed in the process of SPH. Compared with the ST-1 (Sat), the RC of C_9H_{20} and $C_{10}H_{22}$ in ST-3 (Sat) are 1.24 and 1.16 times, respectively. This shows that the occurrence of hydrogen radicals can not only inhibit the aggregation of *n*-alkanes, but also cause the breakage reaction of original asphaltene side chain. Asphaltene aggregation was accelerated to dissociate and the yield of light components was increased. The experimental temperature of SPH is the same as that of TP, the C–C bonds are difficult to break. However, the bond energy of –S– bonds is less than that of C–C bonds. In addition, Table 2 shows that the sulfur content of asphaltene in ST-3 increased from 8.4783 to 8.8394 wt% compared to the feedstock. More sulfur was exposed in the process of dissociation. Therefore, we consider that the dissociation reaction mainly depends on the breakage of –S– bonds at 390 °C. As the carbon number increases, the RC of n-alkanes (≥C12) in ST-3 (Sat) tends to remain stable. It shows that the main type of n-alkanes connected by –S– bonds on asphaltene aggregation is less than $C_{12}H_{26}$.

Naphthalene compounds were analyzed by extracting different characteristic ion fragments. The mass chromatograms of methylnaphthalene compounds are shown in Fig. 7. The corresponding RC can be obtained by Eq. (1). As we can see, the RC of 1-methylnaphthalene in ST-2 (Aro) is only 0.7 times compared

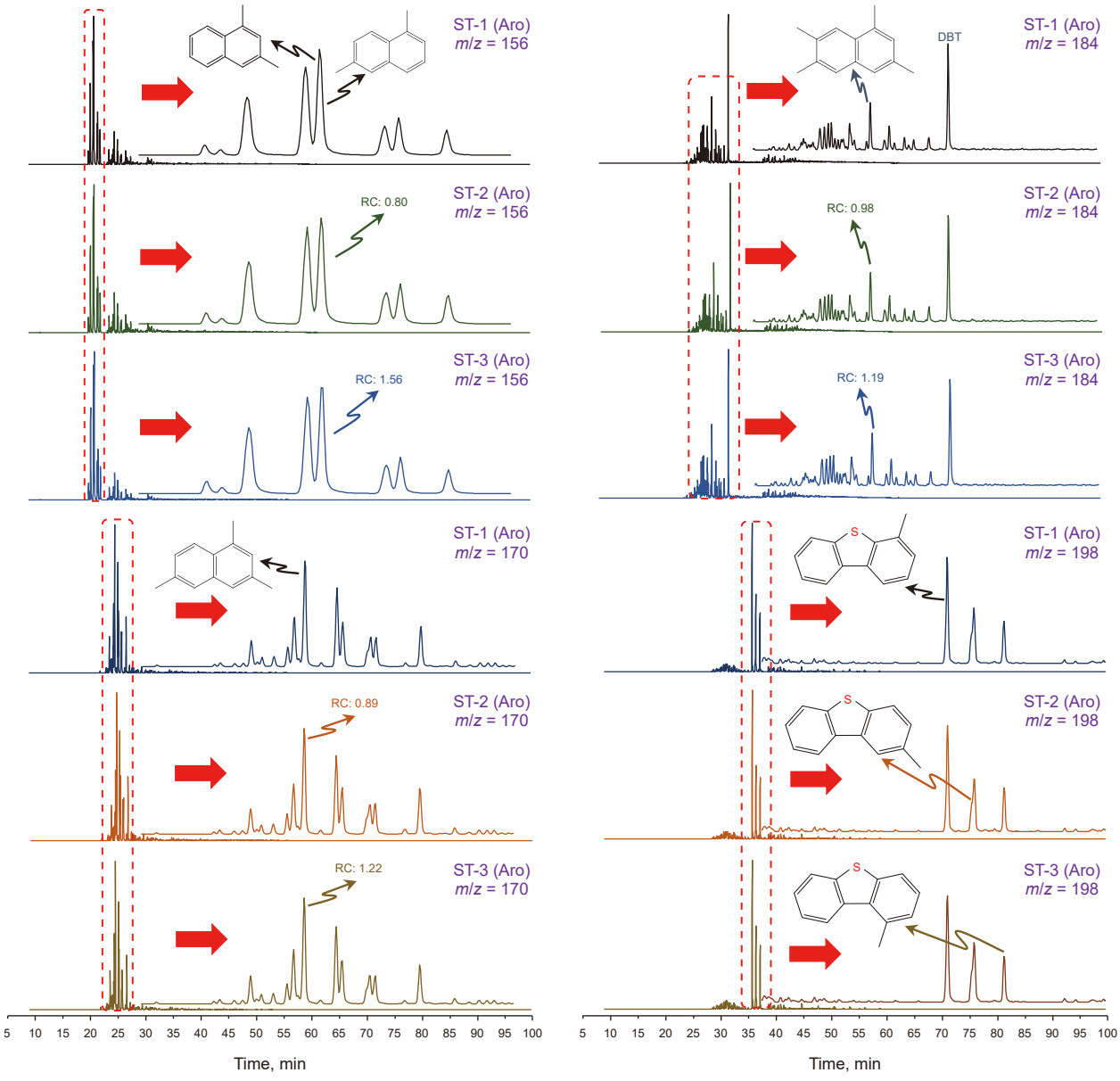

Fig. 8. GC-MS extracted ion chromatograms of naphthalene compounds in aromatics.

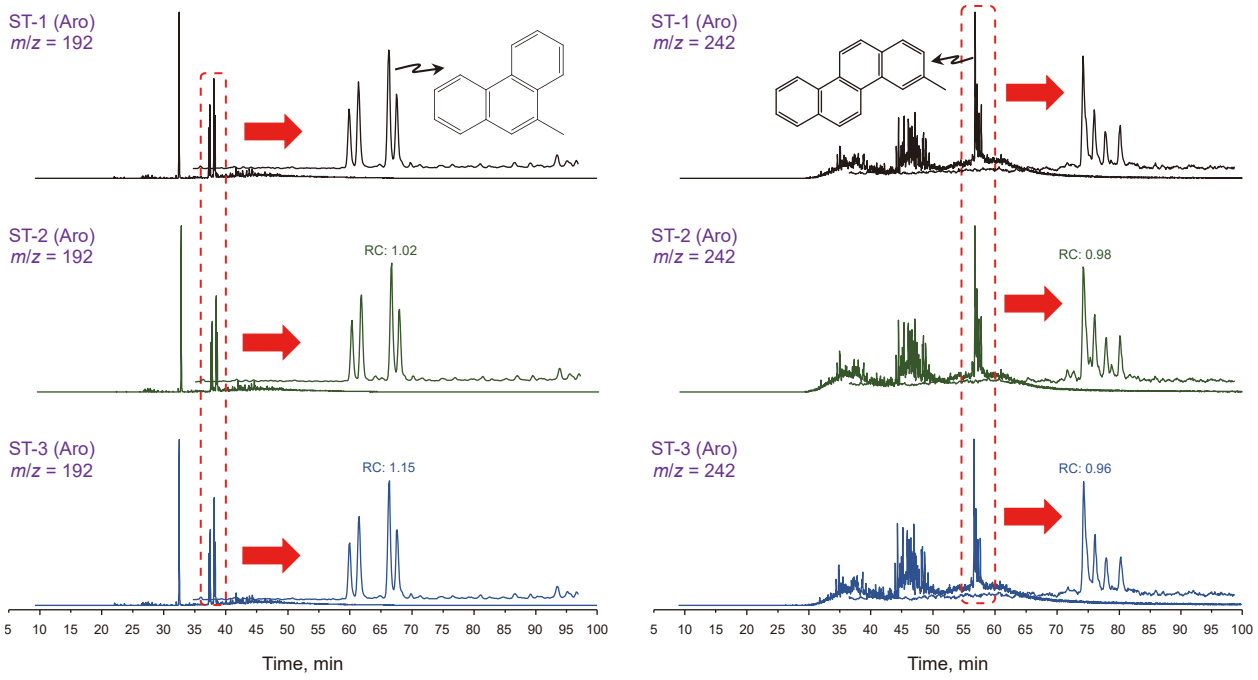

Fig. 9. GC-MS extracted ion chromatograms of methylphenanthrene and methylchrysene.

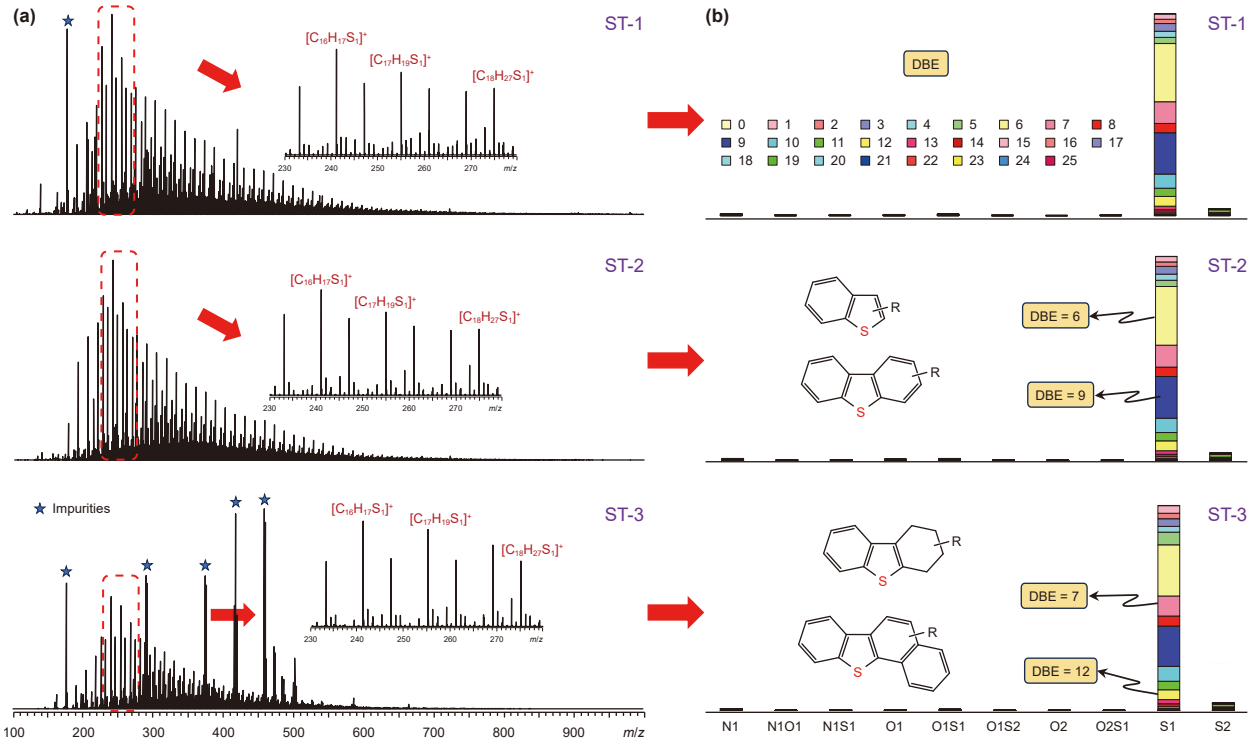

Fig. 10. **(a)** Positive-ion ESI mass spectra of methylation products of the feedstock and processed samples. **(b)** The relative abundance of compound classes assigned from the mass spectra.

with the feedstock and the RC of 2-methylnaphthalene is 0.72 times. Given the temperature of TP, this section of the converted aromatics was difficult to undergo cracking reaction, which also reacted with the radicals of polycyclic aromatic hydrocarbons in asphaltene. Fig. 8 displays other types of naphthalene compounds. We have calculated the RC of the same series of naphthalene

compounds with different structures. The RC of dimethylnaphthalene and trimethylnaphthalene in ST-2 (Aro) are also lower than the feedstock. And the RC of tetramethylnaphthalene in ST-2 (Aro) is consistent with the feedstock. Pentamethylnaphthalene was not detected in both feedstock and processed samples. The conversion efficiency of naphthalene compounds was decreased with the increase of methyl substituent in the process of TP.

In contrast, the RC of naphthalene compounds has been significantly enhanced in the process of SPH. The RC of 1-methylnaphthalene in ST-3 (Aro) is 3.13 times higher than ST-1 (Aro) and the RC of 2-methylnaphthalene is 3.85 times, which are significantly greater than other types of naphthalene compounds. According to the result of SARA separation, the content of ST-3 (Aro) is greater than that of ST-1 (Aro), while the content of ST-3(Asp) is lower than that of ST-1(Asp). This shows that the asphaltene aggregation can undergo hydrocracking to produce small molecular aromatic hydrocarbons at 390 °C in the process of SPH. Methylnaphthalene is the principal compound class generated by dissociation process. In which, the proportion of 2-methylnaphthalene is larger than that of 1-methylnaphthalene. They may be the main structural unit of the outer layer for asphaltene aggregation and pentamethylnaphthalene is the structural boundary. Furthermore, as previously discussed, the dissociation process of asphaltene was achieved by the breakage of –S– bonds. One end of –S– bonds is also connected to naphthalene compounds (including 1-methylnaphthalene, 2-methylnaphtha lene and other naphthalene compounds, etc.).

Fig. 9 shows the variation trend of phenanthrene and chrysene compounds. The influence of the TP and SPH treatments for them appears to be minimal. Compared with the feedstock, the RC of methylphenanthrene and methylchrysene in ST-2 (Aro) are 1.02 and 0.98 times, respectively. Phenanthrene and chrysene compounds can remain stable when heated. It is noteworthy that the RC of methylphenanthrene and methylchrysene in ST-3 (Aro) exhibit a considerable discrepancy. The RC of methylchrysene is 0.96 times that of the feedstock. This means that compounds with four aromatic rings seem to be a boundary for the structure of dissociation products of asphaltene aggregation. For the SPH treatment, the potential reasons for above phenomenon are as follows: 1) The current hydrogenation conditions (390 °C, oil-soluble MoS_2 catalyst) are inadequate for the deep disassembly of asphaltene. Chrysene compounds are located at a greater depth within the asphaltene aggregation than naphthalene compounds. 2) The aromatic hydrocarbon structural units connected in the form of –S– bonds in asphaltene aggregation are dominated by naphthalene compounds.

4.4. Composition and conversion of heteroatom compounds

1) Sulfur compounds

Positive-ion ESI Orbitrap mass spectra and the relative abundance histogram of compound classes for the feedstock and processed samples are shown in Fig. 10. The main type of sulfur compound is S1 species (compounds with one sulfur atom). The distribution of sulfur compounds by the TP treatment is consistent with the feedstock, demonstrating its weak desulfurization performance. For the process of SPH, the relative abundance of sulfur compounds decreased significantly. This is affected by the matrix effect, which is caused by the content change of sulfur compounds.

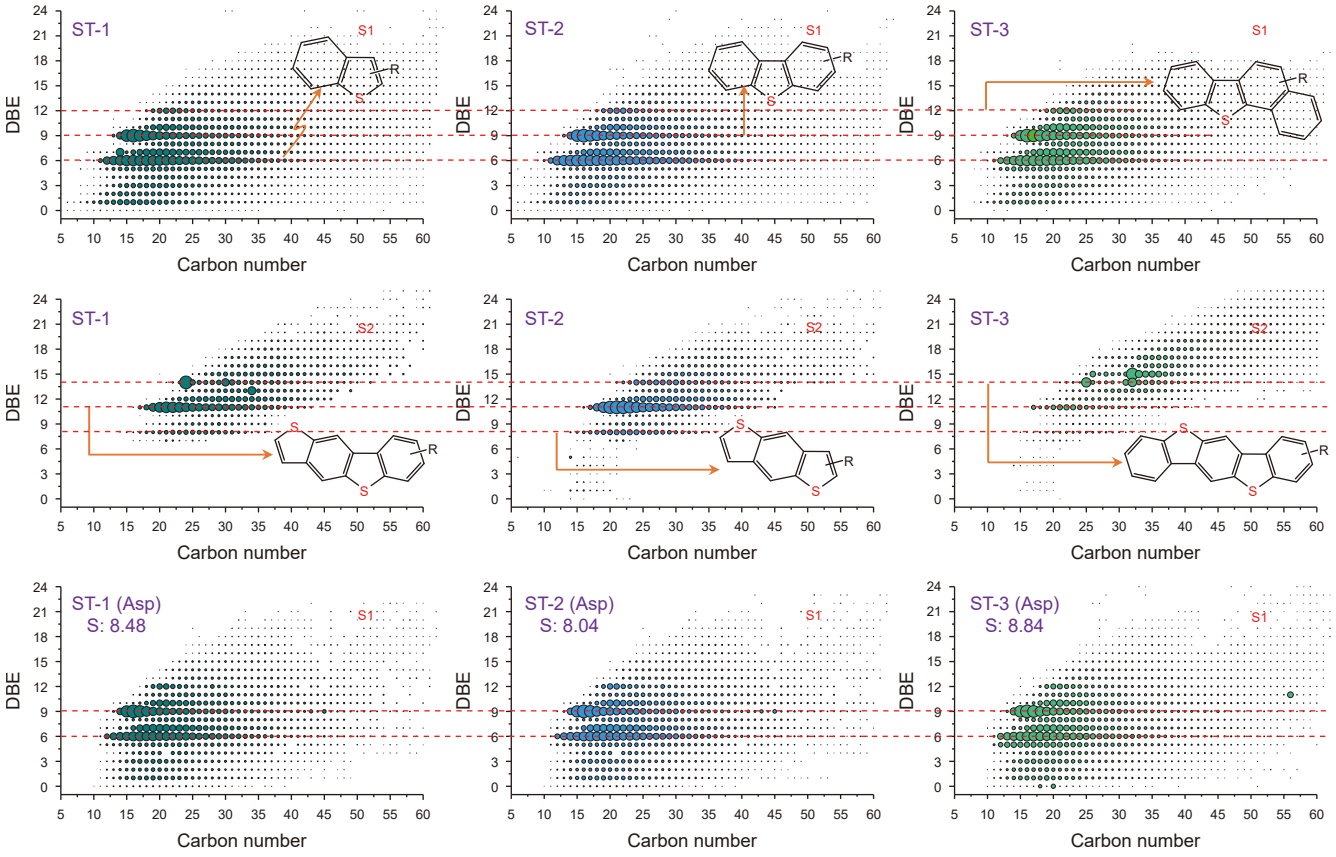

Fig. 11. DBE versus carbon number of S1 and S2 class species for the different samples and their asphaltene components.

In addition, the mass distribution center of ST-3 shifted to the right. It shows that the removal efficiency of small molecular sulfur compounds is higher than that of large molecular. Fig. 11 shows that the DBE versus carbon number distributions of S1 and S2 species. The relative abundance of S1 species with low DBE (<6) decreased in ST-3 but the opposite was true for high DBE (>6). The data indicates that the sulfur compounds with low DBE (mercaptan, thioether and thiophene) are easier to be removed than those with high DBE (benzothiophene, dibenzothiophene). The relative abundance plots of DBE versus carbon number for S2 species (compounds with two sulfur atom) are shown in Fig. 11. We can see that the degree of conversion of S2 species is significantly higher than that of S1 species. This shows that the desulfurization reactivity of S2 species is stronger. And the DBE value distribution of S2 species shows an upward trend in ST-3. And The DBE value of 11 was significantly transformed. The removal effect of S2 species is weaker with the increase of DBE value.

The sulfur compounds in asphaltene were analyzed by ESI Orbitrap MS. The positive-ion ESI mass spectra can be found in Supporting Information. As shown in Fig. 11, the overall relative abundance of sulfide compounds in asphaltene shows an upward trend in ST-3 (Asp) and the sulfur content shows the same characteristics. This phenomenon demonstrates that the existence of –S– bonds in asphaltene and which had a breakage reaction. The content of ionizable sulfur compounds in asphaltene was increased by the process of SPH. The breakage of side chain and the decrease of aromatic ring lamellae can weaken the shielding effect of asphaltene aggregation. Therefore, more detectable sulfur compounds were characterized. In addition, SPH can also act on hydrogen bonds and π–π stacking to achieve the disassembly of asphaltene aggregation, thereby reducing the steric effects and promoting the ionization efficiency of sulfur compounds in ESI.

2) Nitrogen compounds and oxygen compounds

In addition to sulfur compounds, nitrogen compounds and oxygen compounds are also important components of petroleum. Fig. 12 shows that the DBE versus carbon number distributions of these two types of compounds in three samples. There are four class species of compounds, including N1, N2, O1 and O2. For

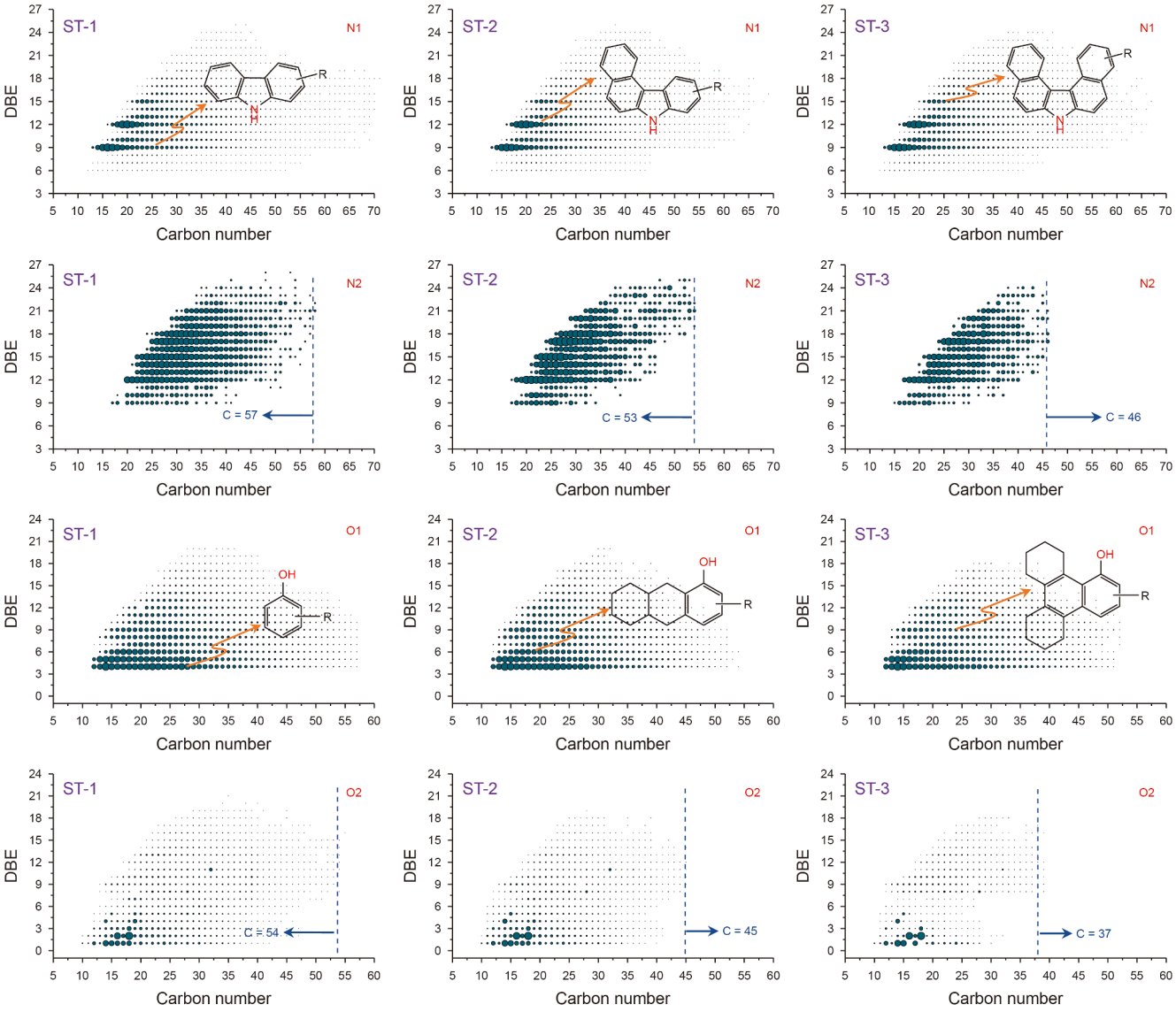

Fig. 12. DBE versus carbon number of nitrogen compounds and oxygen compounds of the different samples.

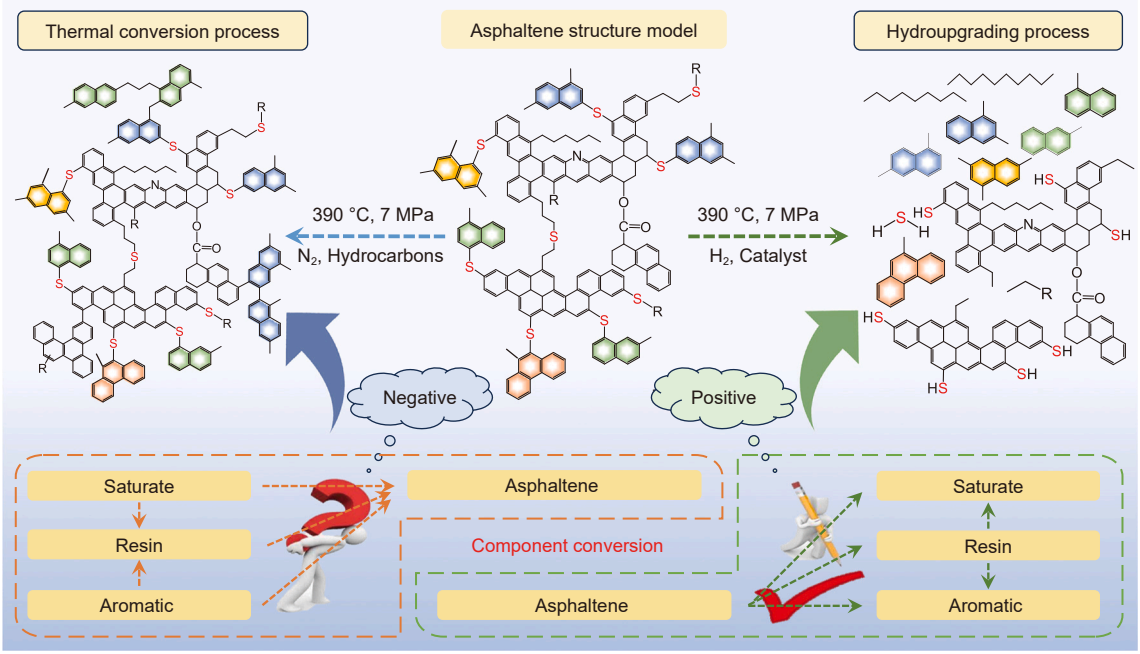

Fig. 13. Schematic of the molecular transformation of asphaltene in Arabian heavy crude oil.

single atom type of heteroatom compounds (N1, O1), no removal effect was observed in both TP and SPH treatments. Compared with the feedstock, the relative abundance of N1 and O1 in ST-2 and ST-3 did not change. On the contrary, the multi-heteroatom compounds (N2, O2) exhibited different characteristics. In the process of TP, we can see that the maximum carbon number distribution of N2 species decreased from 57 to 53. And the O2 species shows the same characteristics, the maximum carbon number distribution decreased from 54 to 45. This indicates that the activity of multi-heteroatom compounds (N2, O2) is significantly higher than that of single heteroatom compounds (N1, O1). In addition, in the previous discussion, we can know that the distribution of S2 species in the process of TP is consistent with the feedstock. It shows that the stability of S2 species is stronger than N2 species and O2 species. On the other hand, in the process of SPH, the multi-heteroatom compounds (N2, O2) were further removed. The maximum carbon number distribution of N2 species and O2 species are only 46 and 37, respectively. The hydrogenation reactivity of N2 species and O2 species with high carbon number is significantly stronger than that of low carbon number. The ability of SPH treatment to remove heteroatom compounds is significantly stronger than that of TP treatment.

4.5. Molecular transformation of asphaltene in different processes

Combined with the above analysis results, the molecular transformation of asphaltene was summarized in Fig. 13. Some n-alkanes and aromatic hydrocarbons underwent condensation reaction with original asphaltene in the process of TP treatment, which led to an increase in the content of asphaltene component. This is something that we do not want to happen in the process of crude oil processing. SPH can not only resolve the above issues but also facilitate further upgrading of crude oil, improving the yield of light components while removing heteroatom compounds. This fully illustrates the necessity of SPH pretreatment for crude oil in refining process. At present, we have obtained a preliminary understanding of the crude oil transform in the process of SPH. Under the conditions of 390 °C and oil-soluble MoS_2 catalyst, the –S– bonds in original asphaltene were broken and small molecular *n*-alkanes, aromatic hydrocarbons and sulfur compounds were generated. Among them, the content of methylnaphthalene changed most obviously. It indicates that methylnaphthalene may be a significant structural unit of asphaltene in Arabian heavy crude oil.

In the next work, we will focus on the upgrading of crude oil processing technology, the design of new catalysts and the in-depth understanding of molecular transformation on this basis. It is our intention to conduct a systematic investigation into the process of crude oil hydrogenation, with a view to providing a practical benefit for actual production.

5. Conclusion

Arabian heavy crude oil was investigated for its TP and SPH pretreatment indicating the superiority of SPH. Combined with a variety of precision analysis methods, the detailed molecular composition of the feedstock and processed samples were characterized. According to the results of basic properties and composition, the understanding of crude oil pretreatment process is as follows:

1) The process of SPH has an excellent lightweight effect for crude oil. While TP increased the asphaltene content of crude oil by about 13.2 wt% compared to the original crude oil, that in the SPH pre-treated crude oil dropped by about 19.8 wt%. Furthermore, SPH provided a much higher yield of distillate fractions than TP. The dissociation of asphaltene is the main factor for crude oil upgrading.
2) Hydroupgrading process mainly generated small molecular *n*-alkanes ($\leq C_{12}H_{26}$) and aromatics (naphthalene and phenanthrene compounds), which are connected to asphaltene by –S– bonds. During the thermal process, not only were the aforementioned compounds not generated, but it also facilitated the condensation between the small molecular hydrocarbons originally present in the crude oil and the asphaltene. The breakage of –S– bonds is the key factor to affect asphaltene

dissociation and methylnaphthalene may be the principal structural units of the outer layer of asphaltene association.

3) For heteroatom compounds, the removal effect of SPH treatment is significantly higher than that of TP treatment. Compared with the single heteroatom compounds (S1, N1 and O1), multi-heteroatom compounds (S2, N2 and O2) exhibited enhanced hydrogenation reactivity. The sulfur compounds (S1, S2) with high DBE are more difficult to remove than those with low DBE; N2 species and O2 species with low carbon number are more difficult to remove than those with high carbon number.

This work systematically investigated the molecular conversion behavior of different processes for crude oil pretreatment. We believe that these detailed characterization result lay an important foundation for in-depth understanding of the key mechanism for improving crude oil utilization efficiency.

CRediT authorship contribution statement

Yi-Di Wang: Writing – original draft. **Xu Zhang:** Investigation. **Xin-Yi Feng:** Investigation. **Bin Liu:** Resources. **Yuan Pan:** Resources. **Guang-Zheng Sun:** Investigation. **Hong-Yang Lv:** Investigation. **Feng-Yu Tian:** Investigation. **Bin Dong:** Resources. **Yi-Chuan Li:** Resources. **Chen-Guang Liu:** Resources. **Yong-Ming Chai:** Writing – review & editing.

Declaration of interests

The authors declare that they have no known competing financial interests or personal relationships that could have appeared to influence the work reported in this paper.

Acknowledgment

This work was supported by grants from the National Natural Science Foundation of China (Nos. U22B20144, 52274308, 22278440 and 22078362), Key R&D Program of Shandong Province, China (No. 2021ZLGX06), and Shandong Provincial Technology Innovation Guidance Plan (No. YDZX2023060).

Appendix A. Supplementary data

Supplementary data to this article can be found online at https://doi.org/10.1016/j.petsci.2025.11.032.

References

Adeyanju, O.A., Oyekunle, L.O., 2019. Experimental study of water-in-oil emulsion flow on wax deposition in subsea pipelines. J. Petrol. Sci. Eng. 182, 106294. https://doi.org/10.1016/j.petrol.2019.106294.

Al-Attas, T.A., Ali, S.A., Zahir, M.H., Xiong, Q., Al-Bogami, S.A., Malaibari, Z.O., Razzak, S.A., Hossain, M.M., 2019. Recent advances in heavy oil upgrading using dispersed catalysts. Energy Fuel 33 (9), 7917–7949. https://doi.org/10.1021/acs.energyfuels.9b01532.

Bello, S.S., Wang, C., Zhang, M., Gao, H., Han, Z., Shi, L., Su, F., Xu, G., 2021. A review on the reaction mechanism of hydrodesulfurization and hydrodenitrogenation in heavy oil upgrading. Energy Fuel 35 (14), 10998–11016. https://doi.org/10.1021/acs.energyfuels.1c01015.

Berg, F.G.A.v.d., 2022. History and review of dual solvent titration methods. Energy Fuel 36 (16), 8639–8648. https://doi.org/10.1021/acs.energyfuels.2c00959.

Bian, H., Xu, F., Kan, A., Wei, S., Zhang, H., Zhang, S., Zhu, L., Xia, D., 2021. Insight into the mechanism of asphaltene disaggregation by alkylated treatment: an experimental and theoretical investigation. J. Mol. Liq. 343, 117576. https://doi.org/10.1016/j.molliq.2021.117576.

Browning, B., Pitault, I., Couenne, F., Jansen, T., Lacroix, M., Alvarez, P., Tayakout-Fayolle, M., 2019. Distributed lump kinetic modeling for slurry phase vacuum residue hydroconversion. Chem. Eng. J. 377, 119811. https://doi.org/10.1016/j.cej.2018.08.197.

Chacón-Patiño, M.L., Rowland, S.M., Rodgers, R.P., 2018. Advances in asphaltene petroleomics. Part 3. Dominance of Island or archipelago structural motif is sample dependent. Energy Fuel 32 (9), 9106–9120. https://doi.org/10.1021/acs.energyfuels.8b01765.

Chen, Y., Lu, Y., Guan, Z., Liu, S., Feng, C., Sun, G., Liang, J., Pan, Y., Liu, C., Liu, Y., 2022. Ultrafine Co-MoS_2 monolayer catalyst derived from oil-soluble single-molecule polyoxometalates for slurry phase hydrocracking. Fuel 315, 123134. https://doi.org/10.1016/j.fuel.2022.123134.

Chen, Z., Wang, Y., Wu, J., Wang, B., Jiang, T., Yu, J., Yang, H., Zhao, S., Shi, Q., Xu, C., 2022. Composition of sulfur species in deasphalted oils and their molecular-level transformation during the hydrotreating process. Fuel 328, 125335. https://doi.org/10.1016/j.fuel.2022.125335.

Deng, S., Li, S., Li, X., 2024. New practical biodegradation proxies based on heteroatom compounds revealed by ESI(−) FT-ICR MS. Org. Geochem. 194, 104815. https://doi.org/10.1016/j.orggeochem.2024.104815.

Dickie, J.P., Yen, T.F., 1967. Macrostructures of the asphaltic fractions by various instrumental methods. Anal. Chem. 39 (14), 1847–1852. https://doi.org/10.1021/ac50157a057.

Feng, W., Zheng, B., Cui, Q., Wang, T., Yuan, P., Zhu, H., Yue, Y., Bao, X., 2022. Influence of ASA composition on its supported Mo catalyst performance for the slurry-phase hydrocracking of vacuum residue. Fuel 324, 124628. https://doi.org/10.1016/j.fuel.2022.124628.

Gray, M.R., Tykwinski, R.R., Stryker, J.M., Tan, X., 2011. Supramolecular assembly model for aggregation of petroleum asphaltenes. Energy Fuel 25 (7), 3125–3134. https://doi.org/10.1021/ef200654p.

Guo, K., Li, H., Yu, Z., 2016. In-situ heavy and extra-heavy oil recovery: a review. Fuel 185, 886–902. https://doi.org/10.1016/j.fuel.2016.08.047.

Hai Pham, H., Hyun Lim, S., Seok Go, K., Sun Nho, N., Hee Kwon, E., Ho Kim, K., Lim, Y.-i., Ryu, H.-J., Park, S.-y., 2022. Modeling and simulation of a bench-scale bubble column reactor for slurry phase hydrocracking of vacuum residue. Fuel 310, 122481. https://doi.org/10.1016/j.fuel.2021.122481.

He, C., Zhang, X., He, L., Sui, H., Li, X., 2022. Revealing the non-covalent interactions between oxygen-containing demulsifiers and interfacially active asphaltenes: a multi-level computational simulation. Fuel 329, 125375. https://doi.org/10.1016/j.fuel.2022.125375.

Kamkar, M., Natale, G., 2021. A review on novel applications of asphaltenes: a valuable waste. Fuel 285, 119272. https://doi.org/10.1016/j.fuel.2020.119272.

Khafaji, H.K., Shahsavand, A., Shooshtari, S.H.R., 2024. Simultaneous optimization of crude oil refinery vacuum distillation column and corresponding ejector system. Energy 294, 130702. https://doi.org/10.1016/j.energy.2024.130702.

Khalaf, M.H., Mansoori, G.A., 2018. A new insight into asphaltenes aggregation onset at molecular level in crude oil (an MD simulation study). J. Petrol. Sci. Eng. 162, 244–250. https://doi.org/10.1016/j.petrol.2017.12.045.

Kovalenko, E.Y., Sagachenko, T.A., Cherednichenko, K.A., Gerasimova, N.N., Cheshkova, T.V., Min, R.S., 2023. Structural organization of asphaltenes and resins and composition of low polar components of heavy oils. Energy Fuel 37 (13), 8976–8987. https://doi.org/10.1021/acs.energyfuels.3c01048.

Law, J.C., Headen, T.F., Jiménez-Serratos, G., Boek, E.S., Murgich, J., Müller, E.A., 2019. Catalogue of plausible molecular models for the molecular dynamics of asphaltenes and resins obtained from quantitative molecular representation. Energy Fuel 33 (10), 9779–9795. https://doi.org/10.1021/acs.energyfuels.9b02605.

Li, L., Jie, H., Mao, R., Li, Y., Chen, G., Yang, Q., Lu, H., 2025. Fast swirl–coalescence filtration: alternative to conventional inclined plate–air flotation for refinery sewage treatment. J. Water Process Eng. 70, 106920. https://doi.org/10.1016/j.jwpe.2024.106920.

Li, S., Wu, J., Wang, Y., Li, Y., Zhang, W., Zhang, Y., He, K., Cai, C., Bian, G., Wang, H., Ji, Y., Shi, Q., 2023. Semi-quantitative analysis of molecular composition for petroleum fractions using electrospray ionization high-resolution mass spectrometry. Fuel 335, 127049. https://doi.org/10.1016/j.fuel.2022.127049.

Li, S., Wu, J., Chen, J., Li, Y., Hu, M., Huang, S., Ren, X., Zhang, W., Zhang, Y., Xu, C., Shi, Q., 2024. Semiquantitative molecular characterization of crude oil. Energy Fuel 38 (5), 3769–3783. https://doi.org/10.1021/acs.energyfuels.3c05086.

Liang, S., Li, X., Wang, C., Guo, X., Jiang, X., Li, Q., Chen, G., Sun, C., 2024. Effect of asphaltenes on growth behavior of methane hydrate film at the oil-water interface. Energy 288, 129734. https://doi.org/10.1016/j.energy.2023.129734.

Liu, B., Zhao, K., Chai, Y., Li, Y., Liu, D., Liu, Y., Liu, C., 2019. Slurry phase hydrocracking of vacuum residue in the presence of presulfided oil-soluble MoS_2 catalyst. Fuel 246, 133–140. https://doi.org/10.1016/j.fuel.2019.02.114.

Liu, B., Lv, H., Cui, X., Sun, G., Zhang, X., Dong, B., Li, Y., Pan, Y., Chai, Y., Liu, C., 2024. Preparation of presulfided oil-soluble NiMo catalyst for slurry bed hydrocracking of vacuum residue. Chem. Eng. J. 498, 155166. https://doi.org/10.1016/j.cej.2024.155166.

Liu, J., Zhao, X., Luo, R., Tao, Z., 2024. A novel link prediction model for interval-valued crude oil prices based on complex network and multi-source information. Appl. Energy 376, 124261. https://doi.org/10.1016/j.apenergy.2024.124261.

Liu, Y., Lu, S., Yan, X., Gao, S., Cui, X., Cui, Z., 2020. Life cycle assessment of petroleum refining process: a case study in China. J. Clean. Prod. 256, 120422. https://doi.org/10.1016/j.jclepro.2020.120422.

Lu, J.M., Wang, Y.F., Zhou, Z.Y., Wu, J.X., Zhang, Y.H., Zhang, L.Z., Shi, Q., He, S.B., Xu, C.M., 2025. Molecular transformation of heavy oil during slurry phase hydrocracking process: influences of operational conditions. Pet. Sci. 22 (2), 884–893. https://doi.org/10.1016/j.petsci.2024.09.002.

Luo, H., Sun, J., Deng, W., Li, C., Du, F., 2022. Preparation of Oil-soluble Fe-Ni sulfide nanoparticles for Slurry-Phase hydrocracking of residue. Fuel 321, 124029. https://doi.org/10.1016/j.fuel.2022.124029.

Marquez, R., Ontiveros, J.F., Nardello-Rataj, V., Sanson, N., Lequeux, F., Molinier, V., 2024. Formulating stable surrogate wood pyrolysis oil-in-oil (O/O) emulsions: the role of asphaltenes evidenced by interfacial dilational rheology. Chem. Eng. J. 495, 153321. https://doi.org/10.1016/j.cej.2024.153321.

Mateus-Rubiano, C., Castillo, A.C., León, P., Rueda, L., Molina V, D., Leon, A.Y., 2024. Effect of hydrotreatment process on the physicochemical properties of a Colombian heavy crude oil post-catalytic aquathermolysis. Energy 298, 131349. https://doi.org/10.1016/j.energy.2024.131349.

Meng, J., Kanike, C., Sontti, S.G., Atta, A., Tan, X., Zhang, X., 2023. Asphaltene precipitation under controlled mixing conditions in a microchamber. Chem. Eng. J. 451, 138873. https://doi.org/10.1016/j.cej.2022.138873.

Mishra, P., Aijaz, T., Yadav, A., 2025. CFD coupled mixing cell network modelling of slurry-phase reactor for vacuum residue hydrocracking. Chem. Eng. J. 503, 157968. https://doi.org/10.1016/j.cej.2024.157968.

Moon, H.-B., Lee, J.-H., Kim, H.-T., Lee, J.-W., Lee, B.-H., Jeon, C.-H., 2024. Effect of high-pressure pyrolysis on syngas and char structure of petroleum coke. Energy 299, 131348. https://doi.org/10.1016/j.energy.2024.131348.

Mullins, O.C., 2010. The modified yen model. Energy Fuel 24 (4), 2179–2207. https://doi.org/10.1021/ef900975e.

Pham, D.D., Nguyen, T.M., Ho, T.H., Le, Q.V., Nguyen, D.L.T., 2024. Advancing hydrodesulfurization in heavy oil: recent developments, challenges, and future prospects. Fuel 372, 132082. https://doi.org/10.1016/j.fuel.2024.132082.

Prajapati, R., Kohli, K., Maity, S.K., 2021. Slurry phase hydrocracking of heavy oil and residue to produce lighter fuels: an experimental review. Fuel 288, 119686. https://doi.org/10.1016/j.fuel.2020.119686.

Rawat, A., Dhakla, S., Maity, S.K., Lama, P., 2024. Mechanistic insight into the coke formation tendency during upgradation of crude oil in slurry phase batch reactor using MoS_2 and its various oil soluble catalysts. Fuel 359, 130433. https://doi.org/10.1016/j.fuel.2023.130433.

Roy, T., Rousseau, J., Daudin, A., Pirngruber, G., Lebeau, B., Blin, J.-L., Brunet, S., 2021. Deep hydrodesulfurization of 4,6-dimethydibenzothiophene over $CoMoS/TiO_2$ catalysts: impact of the TiO_2 treatment. Catal. Today 377, 17–25. https://doi.org/10.1016/j.cattod.2020.05.052.

Shi, Q., Wu, J., 2021. Review on sulfur compounds in petroleum and its products: state-of-the-art and perspectives. Energy Fuel 35 (18), 14445–14461. https://doi.org/10.1021/acs.energyfuels.1c02229.

Shi, Q., Zhang, Y., Chung, K.H., Zhao, S., Xu, C., 2021. Molecular characterization of fossil and alternative fuels using electrospray ionization fourier transform ion cyclotron resonance mass spectrometry: recent advances and perspectives. Energy Fuel 35 (22), 18019–18055. https://doi.org/10.1021/acs.energyfuels.1c01671.

Stratiev, D., Shiskova, I., Toteva, V., Georgiev, G., Dinkov, R., Kolev, I., Petrov, I., Argirov, G., Bureva, V., Ribagin, S., Atanassov, K., Nenov, S., Sotirov, S., Nikolova, R., Veli, A., 2024. Experience in processing alternative crude oils to replace design oil in the refinery. Resources 13 (6), 86. https://doi.org/10.3390/resources13060086.

Su, R., Li, Y., Ma, S., Xiang, H., Wang, Z., Hu, Z., Zhao, Q., Chen, L., Pan, J., Xu, C., Liao, G., Shi, Q., 2023. Evolution of hydrocarbons and carboxylic acids in heavy oil during in situ combustion in Xinjiang oilfield. Energy Fuel 37 (18), 13751–13758. https://doi.org/10.1021/acs.energyfuels.3c02475.

Sun, X., Wang, X., Zhou, J., Zhao, Y., Li, H., Wang, X., Sun, X., Xie, G., 2025. Experimental study of methane-assisted multi-lateral injector SAGD processes as a novel method for extra-heavy oil recovery in heterogeneous reservoirs. Fuel 401, 135939. https://doi.org/10.1016/j.fuel.2025.135939.

Tian, F., Wang, W., Liu, B., Pan, Y., Dong, B., Li, Y., Li, Y., Guo, H., Chai, Y., Liu, C., 2024. Synergistic effect between CoS_x and MoS_2 at the micrometer scale: considerable promotion of the hydrodesulfurization of DBT. Chem. Eng. J. 484, 149579. https://doi.org/10.1016/j.cej.2024.149579.

Usman, A., Aitani, A., Al-Khattaf, S., 2017. Catalytic cracking of light crude oil: effect of feed mixing with liquid hydrocarbon fractions. Energy Fuel 31 (11), 12677–12684. https://doi.org/10.1021/acs.energyfuels.7b02324.

Wang, D., Li, J., Ma, H., Yang, C., Pan, Z., Qu, W., Tian, Z., 2021. Layer-structure adjustable MoS_2 catalysts for the slurry-phase hydrogenation of polycyclic aromatic hydrocarbons. J. Energy Chem. 63, 294–304. https://doi.org/10.1016/j.jechem.2021.08.053.

Wang, L., Guo, J., Li, C., Xiong, R., Chen, X., Zhang, X., 2024. Advancements and future prospects in in-situ catalytic technology for heavy oil reservoirs in China: a review. Fuel 374, 132376. https://doi.org/10.1016/j.fuel.2024.132376.

Wang, Y., Han, X., Gao, Z., Jiang, X., 2022. Thermal cracking of the large molecular alcohols in shale oil by experimental study and kinetic modeling. J. Anal. Appl. Pyrolysis 168, 105749. https://doi.org/10.1016/j.jaap.2022.105749.

Wang, Y., Lu, J., Zhang, X., Zhang, X., Zhang, B., Wu, J., Guan, D., Zhang, Y., Chen, J., Feng, X., Zhang, Y., Zhou, Z., Zhang, L., Shi, Q., 2023a. Molecular transformation of heavy oil during slurry phase hydrocracking process: a comparison between thermal cracking and hydrocracking. Fuel 351, 128981. https://doi.org/10.1016/j.fuel.2023.128981.

Wang, Y., Wu, J., Xie, L., Yuan, M., Jing, Z., Pan, S., Zhang, W., Zhang, Y., Shi, Q., 2023b. Identification and geochemical implication of sulfur compounds in an immature lacustrine shale oil. Energy Fuel. 37 (17), 12946–12952. https://doi.org/10.1021/acs.energyfuels.3c01860.

Wu, J., Zhang, W., Wang, Y., Zhang, Y., Shi, Q., 2023. Identification of sulfur-containing isoprenoids with non-adamantane cage structures in crude oil. Fuel 339, 127390. https://doi.org/10.1016/j.fuel.2023.127390.

Yang, T., Deng, W., Zhu, Y., Zhang, S., Liu, Y., Zhang, X., Yang, C., Li, W., Wang, Y., 2022. The influences of compositional and structural evolutions of asphaltenes on coking behavior during slurry-bed hydrocracking. Fuel 325, 124839. https://doi.org/10.1016/j.fuel.2022.124839.

Yen, T.F., Erdman, J.G., Pollack, S.S., 1961. Investigation of the structure of petroleum asphaltenes by X-ray diffraction. Anal. Chem. 33 (11), 1587–1594. https://doi.org/10.1021/ac60179a039.

Yuan, C., Afanasev, P., Askarova, A., Popov, E., Cheremisin, A., 2025. In situ hydrogen generation in subsurface reservoirs of fossil fuels by thermal methods: reaction mechanisms, kinetics, and catalysis. Appl. Energy 381, 125219. https://doi.org/10.1016/j.apenergy.2024.125219.

Zhao, S., Pu, W., Peng, X., Zhang, J., Ren, H., 2021. Low-temperature oxidation of heavy crude oil characterized by TG, DSC, GC-MS, and negative ion ESI FT-ICR MS. Energy 214, 119004. https://doi.org/10.1016/j.energy.2020.119004.

Zheng, L., Zhao, Q., Dong, Y., Wang, X., Jin, H., Guo, L., 2024. Supercritical water upgrading of heavy oil: effects of reservoir minerals on pyrolysis product distribution. J. Anal. Appl. Pyrolysis 181, 106616. https://doi.org/10.1016/j.jaap.2024.106616.

Zhu, Q., Xu, C., Chen, Q., Wu, L., 2024. Oil price distortion and its impact on green economic efficiency in China's transportation: a spatial effect perspective. Renew. Sustain. Energy Rev. 191, 114148. https://doi.org/10.1016/j.rser.2023.114148.